Enhanced absorption Hanle effect on the $F_{\rm g} = F \rightarrow F_{\rm e} = F + 1$ closed transitions

F. Renzoni[(1)], C. Zimmermann[(2)], P. Verkerk[(3)], and E. Arimondo[(4)]

[(1)] *Institut für Laser-Physik, Universität Hamburg, Jungiusstrasse 9, D-20355 Hamburg, Germany*

[(2)] *Physikalisches Institut, Universität Tübingen, Auf der Morgenstelle 14, D-72076 Tübingen, Germany*

[(3)] *Laboratoire de Physique des Lasers, Atomes et Molécules; U.F.R. de Physique, Université des Sciences et Technologie de Lille, 59655 Villeneuve d'Ascq Cedex, France*

[(4)] *Istituto Nazionale per la Fisica della Materia and Dipartimento di Fisica, Università di Pisa, I-56126 Pisa, Italia*

We analyse the Hanle effect on a closed $F_g \rightarrow F_e = F_g + 1$ transition. Two configurations are examined, for linear- and circular-polarized laser radiation, with the applied magnetic field collinear to the laser light wavevector. We describe the peculiarities of the Hanle signal for linearly-polarized laser excitation, characterized by narrow bright resonances at low laser intensities. The mechanism behind this effect is identified, and numerical solutions for the optical Bloch equations are presented for different transitions.

PACS: 32.80.Qk, 32.80.-t,32.80.Bx

I. INTRODUCTION

Low frequency coherences, between Zeeman or hyperfine split levels, play an important role in laser spectroscopy and quantum optics. Phenomena as coherent population trapping [1], electromagnetic-induced transparency [2], laser without inversion [3], nonlinear susceptibility and refractive index enhancement [4], steep dispersion [5], ultra-low group velocity propagation [6] allow us to realize a coherent control of the absorptive and dispersive properties of an atomic vapor. Zeeman coherences are also a basic ingredient of sub-Doppler [7] and sub-recoil [8] laser cooling mechanisms. Very recently an experimental and theoretical investigation of a multilevel atomic system with two optical fields have revealed a new coherent feature of electromagnetic enhanced absorption [9]. The combined action of the two coherent optical fields produce a low frequency Zeeman coherence that increases the atomic absorption. The subnatural linewidth of the resonance observed scanning the frequency difference between the two optical fields is determined by the coherence relaxation rate. In this work we investigate a closely related enhanced absorption associated to the low frequency Zeeman coherence in a degenerate two level system and detected in a Hanle effect configuration.

In the original Hanle effect [10,11], the resonance fluorescence of an atomic sample is depolarized by an applied magnetic field as result of the destruction of the excited-state Zeeman coherences. In that case the Hanle resonance width is the natural linewidth of the excited state. In the case of the Hanle effect in the ground state [12], the width of the Hanle signal is limited only by the relaxation rate of the ground state and subnatural resonances can be realized. The low-frequency coherences result also in the modification of the total fluorescence intensity, and Hanle resonances of both negative and positive sign have been observed.

The case of a $F_g \rightarrow F_e = F_g, F_g - 1$ transition has been extensively studied [13–16] and more recent work [17,18] has pointed out the strict connection between Hanle effect on these transitions and coherent population trapping. For zero magnetic field the atoms are optically pumped into a nonabsorbing (or dark) state. An applied magnetic field destroys the nonabsorbing state and produces an absorption with a linewidth determined by the relaxation rate of the created Zeeman coherence. Thus the Hanle effect in the ground state of an atomic system appears as a decrease in the atomic absorption, with a minimum centered at zero magnetic field and a linewidth determined by the relaxation rate of the ground state coherences. However anomalous Hanle effect lineshapes may be observed under different experimental conditions. For instance, for the transition $2 \rightarrow 1$ in neon the circulation of Zeeman coherence between excited and ground states produced an inversion in the sign of the Hanle effect, with an increased absorption at zero magnetic field [19].

The study of the Hanle effect on a $F_g \rightarrow F_e = F_g + 1$ transition leads to different results depending whether the considered transition is open or closed. For the *open* $F_g = 1 \rightarrow F_e = 2$ transition of the sodium D_1 line under resonant laser excitation, the fluorescence profile is given by a nearly Lorentzian curve [18]. On the other hand, in the case of the *closed* $F_g = 2 \rightarrow F_e = 3$ transition of the sodium D_2 line line, narrow resonances of positive sign have been observed superposed to the homogeneous broadening Lorentzian profile [20]. Similar observation have been reported also by Fischer and Hertel [21], who explained the effect as a disturbance of the optical pumping process by the Larmor atomic precession. Those authors connected the linewidth of the fluorescence increase to the pumping time, but they did not perform a lineshape investigation. Very recently experimental results of an enhanced absorption in rubidium atoms excited by diode lasers on $F_{\rm g} \rightarrow F_{\rm e} = F_{\rm g} + 1$ transitions have been obtained by two different groups [22,23].

Narrow enhanced-absorption Hanle effect lineshapes have been observed also for in molecules [24], but the mechanism of their production has not been completely defined.

In the present work we analyse the ground-state Hanle effect on a closed $F_{\rm g} \rightarrow F_{\rm e} = F_{\rm g} + 1$ transition, with

the standard configuration of an applied linear-polarized laser radiation and magnetic field collinear to the laser light wavevector. We describe the peculiarities of the Hanle signal for a closed atomic transition, and identify the mechanism responsible for narrow bright resonances at low laser intensities. We provide a connection with the laser cooling processes where ground state coherences play an important role. We derive the lineshape for enhanced absorption Hanle effect with linewidth determined by the ground state optical pumping time. We investigate the bright resonance in the Hanle effect either detected in the fluorescence emission from the absorbing atoms, as in the experiment of Ref. [22], or detected in the light transmitted through the absorbing medium. Similar constrasts for the bright resonance are obtained in the two detection schemes.

The paper is organized as follows. In Section II the theoretical basis of the Optical Bloch Equations (OBE) is introduced. Section III presents an analytical solution of the OBE valid in the limit of weak applied laser electric field. The analytical approach allow us to derive an expression for the enhanced absorption lineshape. Section IV presents numerical solutions valid for different atomic transitions. Finally, in Section V conclusions are drawn.

II. OPTICAL BLOCH EQUATIONS

We consider atoms illuminated by a linearly polarized laser light, resonant with the $F_g \rightarrow F_e$ transition of the D_2 line. As in the standard Hanle effect configuration, a static magnetic field B can be applied collinear to the laser light propagation, the Oz direction. The laser electric field propagating is given by

$$\begin{aligned}\vec{E}(z,t) &= \frac{\mathcal{E}}{2}\vec{\epsilon}_x e^{i(kz-\omega t)} + c.c. \\ &= \frac{\sqrt{2}\mathcal{E}}{4}\left(\vec{\epsilon}_{\sigma^+} + \vec{\epsilon}_{\sigma^-}\right) e^{i(kz-\omega t)} + c.c. \end{aligned} \quad (1)$$

with $\vec{\epsilon}_j$ the unit vector of the j polarization. For comparison, also the case of circularly polarized laser light (say σ^+):

$$\vec{E}(z,t) = \frac{\mathcal{E}}{2}\vec{\epsilon}_{\sigma^+} e^{i(kz-\omega t)} + c.c. \quad (2)$$

will be examined. In writing the optical Bloch equations

$$\dot{\rho} = \frac{1}{i\hbar}\left[H,\rho\right] + \hat{\mathcal{R}}\rho \quad (3)$$

we consider only the contribution to the relaxation operator $\hat{\mathcal{R}}$ due to the spontaneous emission (index SE). By choosing the quantization axis parallel to the magnetic field, the OBEs have the following form ($|e_j\rangle = |J_e, I, F, j\rangle, |g_j\rangle = |J_g, I, F_g, j\rangle$):

$$\begin{aligned}\dot{\rho}_{e_i e_j} &= -[i\omega_{e_i e_j} + \Gamma_{F_e\rightarrow F_g}(1+\alpha_{F_e\rightarrow F_g;F_{g'}})]\rho_{e_i e_j} \\ &\quad + \frac{i}{\hbar}\sum_{g_k}\left(\rho_{e_i g_k} V_{g_k e_j} - V_{e_i g_k}\rho_{g_k e_j}\right) \quad (4a) \\ \dot{\rho}_{e_i g_j} &= -\left[i\omega_{e_i g_j} + \frac{1}{2}\Gamma_{F_e\rightarrow F_g}(1+\alpha_{F_e\rightarrow F_g;F_{g'}})\right]\rho_{e_i g_j} \\ &\quad + \frac{i}{\hbar}\left(\sum_{e_k}\rho_{e_i e_k}V_{e_k g_j} - \sum_{g_k} V_{e_i g_k}\rho_{g_k g_j}\right) \quad (4b) \\ \dot{\rho}_{g_i g_j} &= -i\omega_{g_i g_j}\rho_{g_i g_j} + \frac{i}{\hbar}\sum_{e_k}\left(\rho_{g_i e_k}V_{e_k g_j} - V_{g_i e_k}\rho_{e_k g_j}\right) \\ &\quad + \left(\frac{d}{dt}\rho_{g_i g_j}\right)_{SE}. \quad (4c)\end{aligned}$$

The quantities $\omega_{\alpha_i,\beta_j}$, with $\alpha,\beta = (e,g)$, represent the frequency separation between the energies of levels α_i and β_j,

$$\omega_{\alpha_i,\beta_j} = \frac{E_{\alpha_i} - E_{\beta_j}}{\hbar}, \quad (5)$$

where the energy for the Zeeman level of the ground or excited state with quantum number m_i, including the Zeeman splitting due to the applied magnetic field, is given by

$$E_{\alpha_i} = \delta_{\alpha,e}\hbar\omega_o + g_\alpha \mu_B m_i B. \quad (6)$$

Here g_α represents the gyromagnetic factor of the ground or excited state, and μ_B the Bohr magneton. Γ is the total spontaneous emission rate for any excited level, $\Gamma_{F_e\rightarrow F_g}$ denotes the spontaneous decay rate on the $F_e \rightarrow F_g$ transition and $\alpha_{F_e\rightarrow F_g;F_{g'}}$ the ratio between the spontaneous decays on the $F_e \rightarrow F_{g'}$ and $F_e \rightarrow F_g$ transitions. This ratio is given by

$$\alpha_{F_e\rightarrow F_g;F_{g'}} = \frac{\Gamma_{F_e\rightarrow F_{g'}}}{\Gamma_{F_e\rightarrow F_g}} = \frac{2F_{g'}+1}{2F_g+1}\frac{\left\{\begin{matrix} J_g & F_{g'} & I \\ F_e & J_e & 1\end{matrix}\right\}^2}{\left\{\begin{matrix} J_g & F_g & I \\ F_e & J_e & 1\end{matrix}\right\}^2}. \quad (7)$$

V_{e_k,g_j}, the matrix element of the atom-laser interaction Hamiltonian for linearly polarized laser radiation, in the dipole and rotating wave approximation is given by

$$V_{e_k,g_j} = -\frac{\mathcal{E}}{2}\langle ek|\vec{d}\cdot\vec{\epsilon}_x|gj\rangle e^{-i\omega t} = -\frac{\mathcal{E}\sqrt{2}}{4}\langle ek|d_{+1} + d_{-1}|gj\rangle e^{-i\omega t}. \quad (8)$$

The matrix elements of the spherical components d_q ($q = 0, \pm 1$) of the electric dipole moment can be written as:

$$\begin{aligned}&< J_e, I, F_e, M_e|d_q|J_g, I, F_g, M_g >= \mathcal{D}(-1)^{J_e+I+F_e+F_g-M_e+1}\cdot \\ &\cdot\sqrt{(2F_g+1)(2F_e+1)}\left(\begin{matrix} F_g & 1 & F_e \\ -M_g & q & M_e\end{matrix}\right)\cdot\left\{\begin{matrix} F_e & 1 & F_g \\ J_g & I & J_e\end{matrix}\right\} \quad (9)\end{aligned}$$

where $\mathcal{D} = (J_g||d||J_e)$ is the reduced dipole moment, having indicated with round and curly brackets the $3j$ and $6j$ symbols respectively. The Rabi frequency $\Omega_{\rm R}$ associated to the strongest electric dipole moment for the $F_g \to F_e = F_g + 1$ transition is given by

$$\Omega_{\rm R} = \frac{\sqrt{2}}{2}\frac{\langle J_e, I, F_e, M_e = F_e|d_1|J_g, I, F_g, M_g = F_g\rangle \mathcal{E}}{\hbar}. \tag{10}$$

The spontaneous emission repopulation terms for the density matrix evolution are

$$\left(\frac{d}{dt}\rho_{g_k g_{k'}}\right)_{SE} = (2F_e+1)\Gamma_{F_e\to F_g} \sum_{(q,q'=-F_e,+F_e),(p=-1,1)} (-1)^{p-k-q'} \begin{pmatrix} F_g & 1 & F_e \\ -k & p & q \end{pmatrix} \rho_{e_q e_{q'}} \begin{pmatrix} F_e & 1 & F_g \\ -q' & -p & k' \end{pmatrix}. \tag{11}$$

To eliminate the fast oscillation with the laser frequency ω we introduce the quantities $\tilde{\rho}$ and $\tilde{V}$ defined as:

$$\tilde{\rho}_{e_i e_j} = \rho_{e_i e_j} \tag{12a}$$
$$\tilde{\rho}_{g_i g_j} = \rho_{g_i g_j} \tag{12b}$$
$$\tilde{\rho}_{e_i g_j} = \rho_{e_i g_j} e^{i\omega t} \tag{12c}$$
$$\tilde{V}_{e_i g_j} = V_{e_i g_j} e^{i\omega t}. \tag{12d}$$

Thus the matrix elements $\tilde{V}_{e_i g_j}$ are time-independent and the density-matrix equations in terms of $\tilde{\rho}$ and $\tilde{V}$ can be easily solved numerically.

III. LINESHAPE QUALITATIVE DISCUSSION

As a case study to investigate the linewidth of the bright resonance, we consider an hypothetically closed $F_g = 1 \to F_e = 2$ transition, with Clebsch-Gordon coefficients as in Fig. 1. Moreover we will examine the bright resonance by choosing for the atomic basis two different quantization axis, *i.e.* parallel and perpendicular to the magnetic field direction.

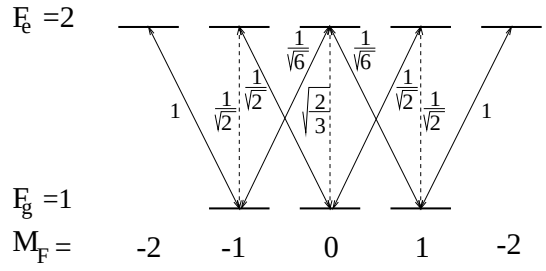

FIG. 1. Interaction scheme for a $F_g = 1 \to F_e = 2$ transition resonant with linearly polarized laser light for two different choices of the atomic basis. For a quantization axis collinear to the light wavevector, the interaction with the light results in σ^+, σ^- excitation (solid lines). For a quantization axis collinear to the light polarization, π-excitation is produced (dashed lines). The Clebsch-Gordan coefficients for the different transitions are reported.

A quick look to the OBE shows that the decay rate for the optical coherences in Eq. (4b), and of the excited state populations and Zeeman coherences in Eq. (4a) is on the order of Γ, the natural width. Thus, in order to modify significantly the excited state populations or coherences related to the excited state, the magnetic field should be strong enough, *i.e.* the Larmor frequency should be on the order of Γ. On the other hand, the natural width does not appear explicitely in Eq. (4c) for the populations and the coherences in the ground state multiplicity. As immediate consequence, the narrow features can be originated from what occurs in the ground state. In the case of a closed transition a steady state can be reached and a particularly simple situation is the limit of weak saturation, where the laser field can be treated as a perturbation. It is well known that in this case the excited state can be adiabatically eliminated, leading to an effective master equation for the density matrix of the ground state [7]. These approximations result in optical coherences proportional to the amplitude of the laser field and excited state populations proportional to the light intensity. The characteristic evolution rate for the ground state populations and coherences is then given by the parameter Γ' known as the optical pumping rate and defined by

$$\Gamma' = \frac{\Gamma}{2}\frac{\Omega_{\rm R}^2}{\delta^2 + \Gamma^2/4}. \tag{13}$$

The choice of the quantization axis is also a crucial point. Clearly, when one introduces a magnetic field, the quantization axis is usually taken along this field. However, because the narrow structures are expected for very weak magnetic fields, a better physical insight can be obtained in the natural basis given, when B=0, by the light polarization. In this basis, the steady state populations for the ground sublevels are $\Pi_{\pm 1} = 4/17$ and $\Pi_0 = 9/17$. The atoms accumulate mostly in the level more interacting with the light field (bright state), leading to a maximum in the fluorescence. When a magnetic field orthogonal to the quantization axis is applied, the populations of the ground states will be partially redistributed, because the Zeeman states are no more eigenstate of the energy for $B \neq 0$. Thus the population of levels weakly coupled to the excited state will increase at the expenses of the population of the bright states. This redistribution, leading to a *decrease* of the fluorescence rate, explains the bright resonance. To couple efficiently the Zeeman sublevels the Larmor frequency has to be of the order of the relaxation rate of the coherences or, in the case of a non-zero laser detuning, of the order of the energy separation due to the light-shift. Because the relaxation rate of the coherences is Γ', a narrow feature is expected, even if a more careful examination is needed to give the proportionality coefficient. Notice also the strong analogy with the Raman spectroscopy of $\sigma^+ - \sigma^-$ optical molasses, where a two-photon process couples the Zeeman sublevels [25].

If the magnetic field is used as quantization axis, a different description of the process originates with a creation

of Zeeman ground state coherence at zero magnetic field and its destruction at non zero values of magnetic fields characterizing the bright resonance. In fact the density matrix investigation required to analyse the Hanle effect with quantization axis along the magnetic field direction is formally equivalent to that of the polarization gradient mechanism denominated as $\sigma^+ - \sigma^-$ configuration. In [7] it was shown that the equivalence is realized by replacing the atomic Larmor frequency in the applied magnetic field with the Doppler shift of the atoms moving within the cooling laser field. Thus the equations derived for the ground-state populations and coherences in those references eliminating adiabatically the optical coherences and the excited-state populations and coherences may be used to analyze the coherence creations in the bright line Hanle effect. Let $C_{\rm r}$ and $C_{\rm i}$ be the real and imaginary parts of the ground state coherence $\tilde{\rho}_{g_1 g_{-1}}$

$$\tilde{\rho}_{g_1 g_{-1}} = C_r + iC_i \tag{14}$$

and let Π_i be the ground state populations

$$\Pi_i = \rho_{g_i g_i} \tag{15}$$

For a weak laser intensity, such that the adiabatic eliminations can be applied, the equivalence with the analysis of ref. [7] allows us to write a closed set of five equations for the ground state populations and coherences

$$\dot{\Pi}_1 = -\frac{5\Gamma'}{72}\Pi_1 + \frac{9\Gamma'}{72}\Pi_0 + \frac{\Gamma'}{72}\Pi_{-1} - \frac{\Gamma'}{18}C_r - \frac{\delta'}{6}C_i \tag{16a}$$

$$\dot{\Pi}_{-1} = \frac{\Gamma'}{72}\Pi_1 + \frac{9\Gamma'}{72}\Pi_0 - \frac{5\Gamma'}{72}\Pi_{-1} - \frac{\Gamma'}{18}C_r + \frac{\delta'}{6}C_i \tag{16b}$$

$$\dot{\Pi}_0 = -\dot{\Pi}_{-1} - \dot{\Pi}_1 \tag{16c}$$

$$\dot{C}_r = \frac{\Gamma'}{24}\Pi_1 + \frac{\Gamma'}{8}\Pi_0 + \frac{\Gamma'}{24}\Pi_{-1} - \frac{5\Gamma'}{12}C_r + \frac{2\mu_g B}{\hbar}C_i, \tag{16d}$$

$$\dot{C}_i = \frac{\delta'}{12}\left(\Pi_1 - \Pi_{-1}\right) - \frac{2\mu_g B}{\hbar}C_r - \frac{5\Gamma'}{12}C_i. \tag{16e}$$

where we have introduced the light shift δ'

$$\delta' = \frac{\omega - \omega_o}{2}\frac{\Omega_R^2}{\delta^2 + \Gamma^2/4} \tag{17}$$

and $\mu_g = g_g \mu_B$. Introducing the population difference $d = \Pi_1 - \Pi_{-1}$ and using the relation $\Pi_{-1} + \Pi_1 = 1 - \Pi_0$, Eqs. (16) may be rewritten as

$$\dot{d} = -\frac{\Gamma'}{12}d - \frac{\delta'}{3}C_i, \tag{18a}$$

$$\dot{\Pi}_0 = \frac{\Gamma'}{18} - \frac{11\Gamma'}{36}\Pi_0 + \frac{\Gamma'}{9}C_r, \tag{18b}$$

$$\dot{C}_r = \frac{\Gamma'}{24} + \frac{\Gamma'}{12}\Pi_0 - \frac{5\Gamma'}{12}C_r + \frac{2\mu_g B}{\hbar}C_i, \tag{18c}$$

$$\dot{C}_i = \frac{\delta'}{12}d - \frac{2\mu_g}{\hbar}BC_r - \frac{5\Gamma'}{12}C_i. \tag{18d}$$

whose steady state solution is

$$C_r = \frac{5}{34}\left[1 + \frac{132}{17}\frac{\left(\frac{4\mu_g B}{\hbar}\right)^2}{4\left(\delta'\right)^2 + 5\left(\Gamma'\right)^2}\right]^{-1}, \tag{19a}$$

$$\Pi_0 = \frac{2}{11}(1 + 2C_r), \tag{19b}$$

$$C_i = -\frac{24\mu_g B}{\hbar}\frac{\Gamma'}{4\left(\delta'\right)^2 + 5\left(\Gamma'\right)^2}C_r, \tag{19c}$$

$$d = -4\frac{\delta'}{\Gamma'}C_i. \tag{19d}$$

The fluorescence signal is proportional to the total excited state population. In the low saturation limit, the population of each excited state may be expressed as a function of the ground state quantities [7]

$$\rho_{e_{\pm 2}e_{\pm 2}} = \frac{1}{4}\frac{\Omega_R^2}{\delta^2 + \Gamma^2/4}\Pi_{\pm 1}, \tag{20a}$$

$$\rho_{e_{\pm 1}e_{\pm 1}} = \frac{1}{8}\frac{\Omega_R^2}{\delta^2 + \Gamma^2/4}\Pi_0, \tag{20b}$$

$$\rho_{e0e0} = \frac{1}{2}\frac{\Omega_R^2}{\delta^2 + \Gamma^2/4}\left[\frac{1}{12}\left(\Pi_1 + \Pi_{-1}\right) + \frac{1}{6}C_r\right]. \tag{20c}$$

The total excited state population at the steady state Π_{st}^e is

$$\Pi_{st}^e = \sum_{i=-2,2}\rho_{e_i e_i} = \frac{\Omega_R^2}{\delta^2 + \Gamma^2/4}\left(\frac{25}{88} + \frac{3}{44}C_r\right). \tag{21}$$

Thus the variation in the fluorescence with the magnetic field is associated to the modification of the ground state coherence with the magnetic field. The laser interaction produces a large coherence, 5/34, between the $m_F = -1$ and $m_F = 1$ Zeeman sublevels. Increasing the magnetic field the coherence C_r is reduced from its maximum value at $B = 0$ to zero. The equation for C_r represents a narrow bright resonance whose HWHM ΔB is

$$\Delta B = \frac{\hbar}{8\mu_g}\sqrt{\frac{17}{33}\left[4\left(\delta'\right)^2 + 5\left(\Gamma'\right)^2\right]}. \tag{22}$$

The contrast C, defined as the amplitude of the narrow resonance divided by the amplitude of the homogenous broadened line, is 3/85, independent of the Rabi frequency and laser detuning in the limit of low-saturation. Note however that the Rabi frequency and laser detuning determine the time scale to reach the steady state, as from the Eq. (13) for Γ'.

On the other hand, when the polarization of the light is circular, the population accumulates in the m=+1 sublevel and a magnetic field along the quantization axis does not redistribute the populations. As a consequence, one expects no narrow structures in the case of a circularly polarized beam with a magnetic field along the propagation axis.

IV. NUMERICAL SOLUTION OF THE OBE

To point out out the basic features of the effect of narrow bright resonances, we have solved the OBE for a cold atomic sample, where the laser light excites only one atomic hyperfine transition, with only the natural broadening. Moreover for a cold sample the interaction time between laser and atoms may be assumed long enough to consider only the steady state solution of the density matrix equations.

The bright line has been detected either on the fluorescent light emitted by the atomic sample as in experiment of Ref. [22], or on the light transmitted by the atomic sample, as in the experimental results reported in Ref. [23]. For the fluorescence measurements the bright line appear as an increase of the emitted light. For the transmission measurements the bright line appears as an additional loss, *i.e.* as a reduced transmission, and an increase in absorption. For a laser excited closed transition, the atoms reach a steady state, and the fluorescence intensity $I(B)$ emitted from the cold atomic sample interacting with the laser beam is proportional to the steady state total population of the excited state Π^e_{st}. Thus the dependence of this quantity on the amplitude of the applied magnetic field produces the Hanle effect lineshapes observed on the fluorescence emission. For the transmission measurements, we characterize the transmission signal T by considering the imaginary part $\chi^{''}$ of the susceptibility, *i.e.* the loss per unit wavelength.

A. Closed Rb D_2 line transitions

We have examined the bright line Hanle signals for both the $F_g = 2 \rightarrow F_e = 3$ D_2 transition of the the ^{87}Rb isotope and for the $F_g = 3 \rightarrow F_e = 4$ D_2 transition of the ^{85}Rb isotope, with similar results in the two cases. Results of the numerical calculation for the total stationary excited-state population $\Pi^e_{st}(B)$ for ^{87}Rb are reported in Fig. 2 at different laser intensities. Results of the numerical calculation for the susceptibility χ'' in the case of the $F_g = 3 \rightarrow F_e = 4$ D_2 transition of the the ^{85}Rb isotope are reported in Fig. 3 also for different laser intensities. In both cases for comparison also the results for circularly polarized laser light have been reported as dashed lines. In the case of linearly polarized laser light, for small laser intensities a narrow bright resonance appears around $B = 0$, in both fluorescence emission and transmission, superposed to a broader line. That narrow feature is more clearly shown in the insets, and is absent in the case of circularly polarized laser field. The contrast C of the bright resonance is around ten percent for both detection schemes and is nearly independent of the laser intensity up to intensities of 0.1 mW/cm^2. At larger laser intensities the contrast decreases. Furthermore the bright resonance disappears at laser intensities around few mW/cm^2.

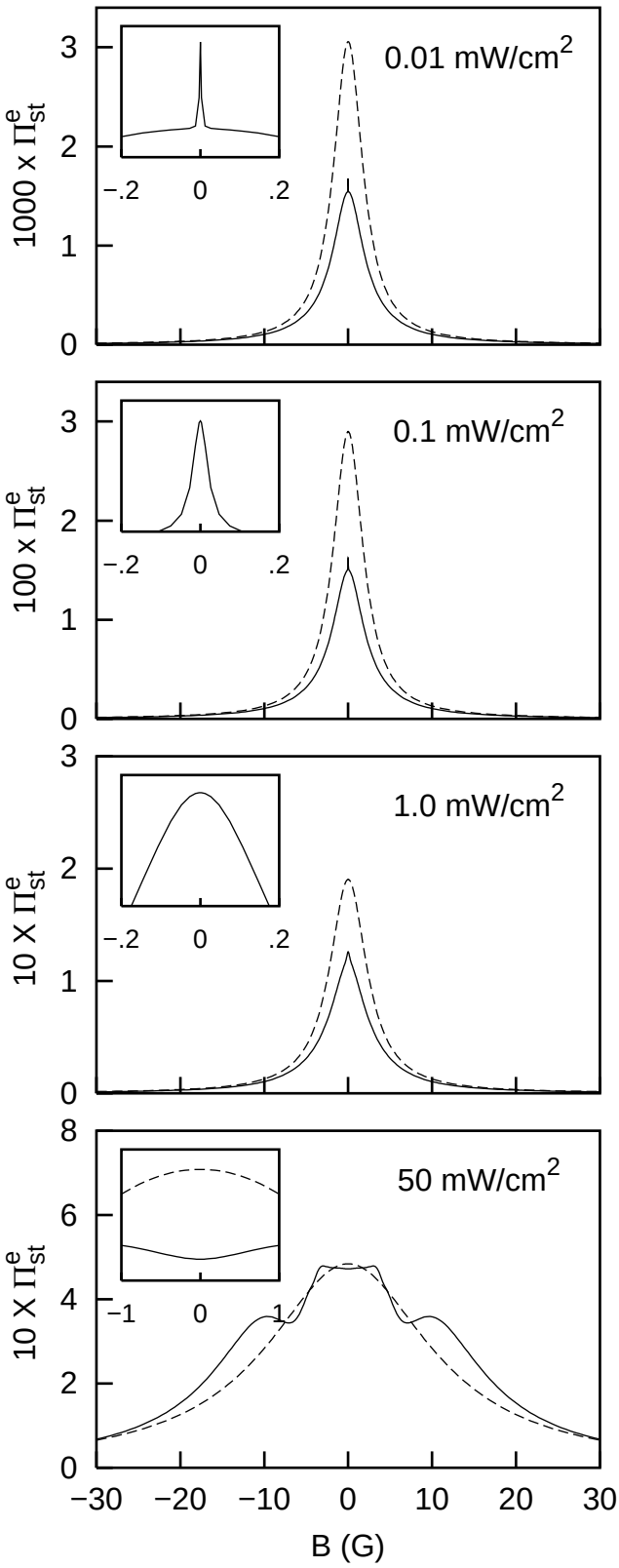

FIG. 2. Steady-state total population of the excited state as a function of the applied magnetic field for different laser intensities. The calculations refer to the $F_g = 2 \rightarrow F_e = 3$ transition of the ^{87}Rb D_2-line. Solid lines correspond to linearly polarized laser light, dashed line to circular polarization. The insets evidence the regions around zero magnetic field.

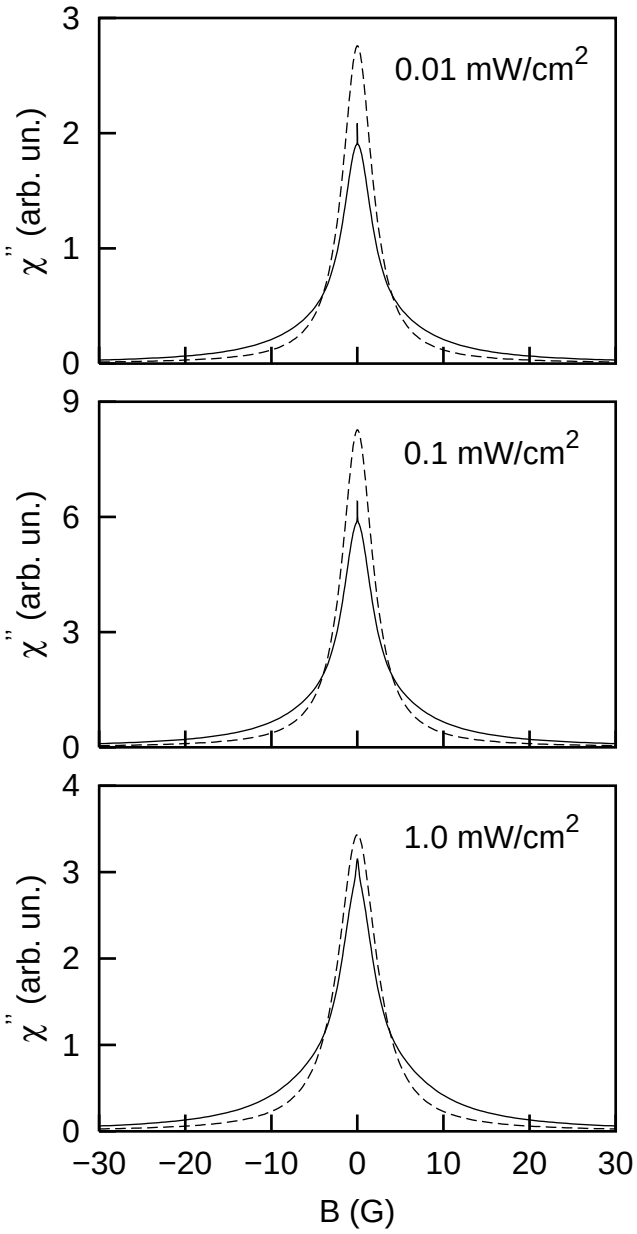

FIG. 3. Imaginary part of the total susceptibility versus the magnetic field B for different laser intensities in the case of the $F_g = 3 \rightarrow F_e = 4$ transition of the ^{85}Rb D_2-line. Solid lines correspond to linearly polarized laser light, dashed line to circular polarization.

At high laser intensities, the distribution of the population in the ground state is irrelevant. It is important instead the number of excited-state levels which can be effectively populated. For zero magnetic field, the two Zeeman levels edges of the excited state, with $M_e = \pm 3$, are not populated and all the allowed transitions $|g, i\rangle \rightarrow |e, i\rangle$ are saturated, producing $\rho_{g_i g_i} \simeq \rho_{e_i e_i}$. Therefore the total fluorescence intensity $I(0)$ becomes

$$I(0) = \Gamma \sum_{i=-2,2} \rho_{e_i e_i} \simeq \frac{\Gamma}{2} \left(\sum_{i=-2,2} \rho_{e_i e_i} + \sum_{i=-2,2} \rho_{g_i g_i} \right) = \frac{\Gamma}{2} \tag{23}$$

independent of the distribution of the atomic population. For non-zero magnetic field also the two Zeeman edge states can be occupied as a result of the magnetic-field mixing between excited state sublevels, so the total excited-state population can increase. This explain the high-intensity reversed lineshape appearing in Fig. 2.

B. Open $F_g = 1 \rightarrow F_e = 2$ transition of the ^{87}Rb D_2-line

We consider now the open $F_g = 1 \rightarrow F_e = 2$ transition of the ^{87}Rb D_2-line. For a laser excited open transition, the stationary excited-state population is zero [18], and the fluorescence intensity $I_{\rm int}(B)$ emitted from the atomic sample within the interaction time $t_{\rm int}$ depends on the time integrated total population $\Pi^e_{\rm int}(B)$ of the excited state defined by

$$I_{\rm int}(B) = \Gamma \Pi^e_{\rm int}(B) = \Gamma \int_0^{t_{\rm int}} \Pi^e(B, t) dt. \tag{24}$$

By numerically solving the optical Bloch equation, we calculated the integrated excited-state population $\Pi^e_{\rm int}$, Eq. (24), as reported in Fig. 4. The plots indicate that in this case there is no bright resonance. Such a result is in agreement with that of Akulshin *et al* [9] derived for a bichromatic configuration: subnatural resonances do not occurr in open transitions. In fact, as discussed previously, the phenomenon of bright resonances corresponds to the redistribution, via optical pumping, of the population in the ground state with an accumulation into the levels maximally coupled to the excited state. The presence of a channel of decay out of the levels excited by the laser contrasts this accumulation: the strong transitions are depleted at a higher rate than the weak ones. For a loss rate large enough, the depletion dominates and no bright resonance occurs. Finally, for sufficiently large interaction times and laser intensities, the atomic states are completely depleted by the laser.

The analysis of Ref. [18] has shown that the time-integrated excited-state population depends only on the loss parameter $\alpha_{F_e=2 \rightarrow F_g=1;F_{g'}}$, and is independent of the magnetic field, for a range within the homogeneous linewidth. The flat spectra of Fig. 4 at large laser intensities are produced by those dependencies.

C. Closed $F_g = 4 \rightarrow F_e = 5$ transition of the Cs D_2-line

In the work of Théobald *et al* [16] the Hanle effect on the different hyperfine transitions of the Cs D_2-line was investigated for applied linearly-polarized broadband laser radiation. Their result for the closed $F_g = 4 \rightarrow F_e = 5$ transition is, at first sight, in disagreement with our general conclusion for a $F_g = F \rightarrow F_e = F + 1$ transition.

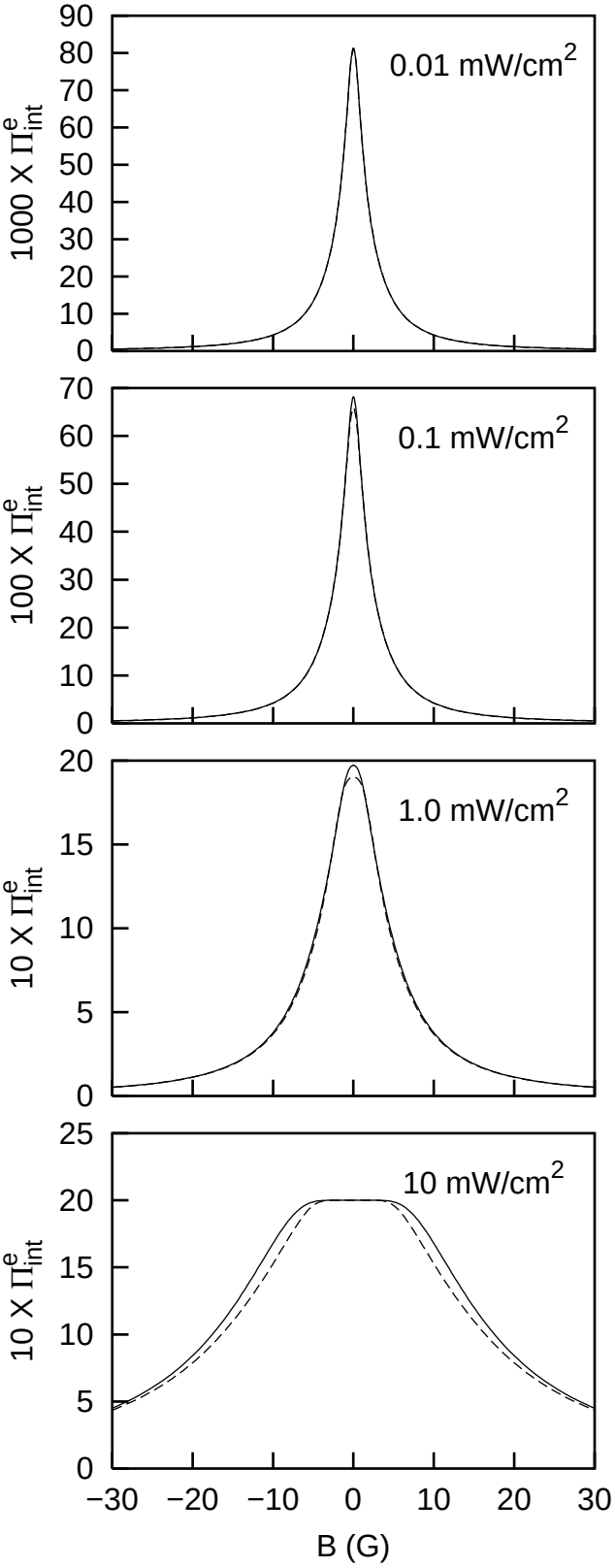

FIG. 4. Total population of the excited state integrated over an interaction time $t_f = 100\Gamma$ as a function of the applied magnetic field for different laser intensities. The calculations refer to the $F_g = 1 \rightarrow F_e = 2$ transition of the ^{87}Rb D_2-line. Solid lines correspond to linearly polarized laser light, dashed line to circular polarization.

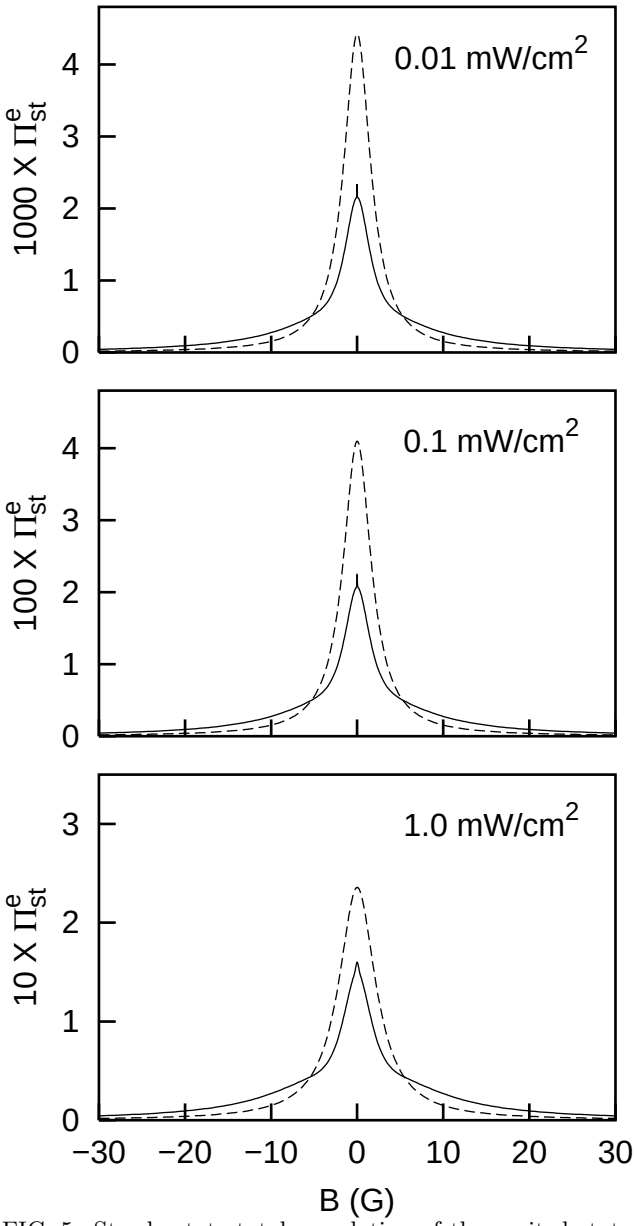

FIG. 5. Steady-state total population of the excited state as a function of the applied magnetic field at different laser intensities, for the $F_g = 4 \rightarrow F_e = 5$ transition of the Cs D_2-line. Solid lines correspond to linearly polarized laser light, dashed line to circular polarization.

In fact in that experiment the measured intensity of the fluorescence from the atomic sample was almost constant around zero magnetic field, for a laser intensity of 2 mW/cm^2 and an interaction time of 12 μs. In order to clarify this point, we solved the optical Bloch equations also for the $F_g = 4 \rightarrow F_e = 5$ closed transition of the cesium D_2 line. Results for Π^e_{st} are shown in Fig. 5.

The dependence of the excited-state population on the magnetic field at different laser intensities and polarizations is completely analogous to the behaviour observed for the closed $F_g = F \rightarrow F_e = F + 1$ transition of the

^{85}Rb and ^{87}Rb, therefore confirming the general validity of this behaviour. However the results of Fig. 5 clarify why in the experiment of Théobald *et al* the fluorescence intensity was almost constant around zero magnetic field: in the experimental investigation the laser intensity was beyond the low-saturation regime, in which sharp bright resonances occur.

V. CONCLUSIONS

We studied theoretically the Hanle effect on closed $F_g = F \to F_e = F + 1$ transitions. Both cases of linear- and circular-polarized laser excitation have been considered. An analytic solution of the optical Bloch equations has been given for a closed $F_g = 1 \to F_e = 2$ transition. Numerical solutions have been obtained for the transitions corresponding to available experimental data.

For the examined closed transitions resonant with a linear polarization laser field, bright resonances, *i.e.* sharp increases of the absorption have been reproduced around zero magnetic field at low laser intensities. The enhanced absorption corresponds to the accumulation, via optical pumping, of the atomic population in the ground states maximally coupled to the excited state. The application of a magnetic field perpendicular to the light polarization redistributes the population among the ground state sublevels, and results in a decrease of the fluorescence intensity. At increasing intensities of the linear-polarized laser field, the strength of the bright resonance is progressively reduced, and in the saturation regime of the optical transition a decrease of the absorption around zero magnetic field is produced.

Our calculations for open transitions have confirmed that the bright resonance does not generally occurs for this kind of transitions. In effect for open transitions the laser field will empty the ground state with a rate similar to that needed to redistribute the ground state population. Furthermore it should be pointed out that the bright-line production requires an optical pumping process. Thus, depending on the applied laser intensity, the interaction time should be long enough to let the atoms reach their steady state. For instance, the steady state was not reached in Ref. [20] where it was demonstrate that for sufficiently weak light intensities the bright resonance disappears, because the redistribution of the population in the ground state was not achieved.

ACKNOWLEDGMENTS

We thank S.S. Cartaleva and G. Alzetta for showing us their results prior to publication. F.R. thanks A. Hemmerich for many useful discussions and the Deutsche Forschungsgemeinschaft for financial support under project Li 417/4-1. The *Laboratoire de Physique des Lasers, Atomes et Molécules* is a *Unité Mixte de Recherche de l'Université de Lille 1 et du CNRS*.

[1] For a review see E. Arimondo, in Progress in Optics ed. E. Wolf, vol. 35 (Elsevier, Amsterdam, 1996) p. 257.

[2] S. E. Harris, Physics Today **50**, 36 (1997). See also M.O. Scully and M.S. Zubairy, *Quantum Optics*, (University Press, Cambridge, 1997).

[3] A.S. Zibrov, M.D. Lukin, D.E. Nikonov, L. Hollberg, M.O. Scully, V.L. Velichansky, and H.G. Robinson, Phys. Rev. Lett. **75**, 1499 (1995).

[4] S.E. Harris, J.E. Field, and A. Imamoglu, Phys. Rev. A **64**, 107 (1990); A.S. Zibrov, M.D. Lukin, L. Hollberg, D.E. Nikonov, M.O. Scully, H.G. Robinson, and V.L. Velichansky, Phys. Rev. Lett. **76**, 3935 (1996).

[5] Y.-Q. Li and M. Xiao, Phys. Rev. A **51**, R2703 (1995); O. Schmidt, R. Wynands, Z. Hussein and D. Meschede, Phys. Rev. A **53**, R27 (1996); S. Brandt, A. Nagel, R. Wynands and D. Meschede, Phys. Rev. A **56**, R1063 (1997); S. Brattke, U. Kallmann and W.-D. Hartmann, Eur. Phys. J. D **3**, 159 (1998).

[6] L.V. Hau, S.E. Harris, Z. Dutton and C. H. Behroozi, Nature **397**, 594 (1999); M. M. Kash, V. A. Sautenkov, A. S. Zibrov, L. Hollberg, G. R. Welch, M. D. Lukin, Y. Rostovtsev, E.S. Fry and M. O. Scully, Phys. Rev. Lett. **82**, 5229 (1999); D. Budker, D.F. Kimball, S.M. Rochester, and V.V. Yashchuk, Phys. Rev. Lett. **83**, 1767 (1999).

[7] J. Dalibard and C. Cohen-Tannoudji, J. Opt. Soc. Am. B **6**, 2023 (1989); C. Cohen-Tannoudji, in *Fundamental Systems in Quantum Optics*, eds. J. Dalibard, J.M. Raimond, J. Zinn-Justin (Elsevier Science, 1991).

[8] A. Aspect, E. Arimondo, R. Kaiser, N. Vansteenkiste, and C. Cohen-Tannoudji, Phys. Rev. Lett. **61**, 826 (1988).

[9] A.M. Akulshin, S. Barreiro, and A. Lezama, Phys. Rev. A **57**, 2996 (1998); A. Lezama, S. Barreiro, and A.M. Akulshin, *ibidem* **59**, 4732 (1999); and A.M. Akulshin, S. Barreiro, and A. Lezama, Phys. Rev. Lett. **83**, 4277 (1999).

[10] For an introduction to the Hanle effect see A. Corney *Atomic and Laser Spectroscopy* (Oxford University Press 1977).

[11] The book G. Moruzzi and F. Strumia eds. *The Hanle effect and level-crossing spectroscopy*, (Plenum, New York, 1991) contains a selection of papers on the Hanle effect.

[12] J. Dupont-Roc, S. Haroche and C. Cohen-Tannoudji, Phys. Lett. **28A**, 638 (1969); C. Cohen-Tannoudji, J. Dupont-Roc, S. Haroche and F. Laloë, Phys.Rev. Lett. **22**, 758 (1969).

[13] J.L. Picqué, J. Phys. B **11**, L59 (1978).

[14] G. Bertuccelli, N. Beverini, M. Galli, M. Inguscio, F. Strumia and G. Giusfredi, Opt. Lett. **10**, 270 (1985).

[15] R.J. McLean, R.J. Ballagh and D.M. Warrington, J. Phys. B **18**, 2371 (1985).

[16] G. Théobald, N. Dimarco, V. Giordano and P. Cerez,

Opt. Comm. **71**, 256 (1989).
[17] V.S. Smirnov, A.M. Tumaikin, and V.I. Yudin, Zh. Eksp. Teor. Fiz. **96**, 1613 (1989) [JETP **69**, 913 (1989)].
[18] F. Renzoni, W. Maichen, L. Windholz, and E. Arimondo, Phys. Rev. A**55**, 3710 (1997); F. Renzoni and E. Arimondo, Phys. Rev. A **58**, 4717 (1998).
[19] M.P. Gorza, B. Decomps, and M. Ducloy, Opt. Commun. **8**, 323 (1973); M. Ducloy, Ann. Phys. (France) **8**, 403 (1973).
[20] H. Brand, W. Lange, J. Luther, B. Nottbeck and H.W. Schröder, Opt. Comm. **13**, 286 (1975).
[21] A. Fischer and I.V. Hertel, Z.Phys. A-Atoms and Nuclei **304**, 103 (1982).
[22] Y. Dancheva, G. Alzetta, S. Cartaleva, M. Taslakov, and Ch. Andreeva, Opt. Comm. **178**, 103 (2000).
[23] S.-S. Beyertt, Master thesis, Tübingen (2000).
[24] H.G. Weber in Ref. [11] pag. 87.
[25] J.-Y. Courtois, Ann. Phys. Fr., **21**, pp. 1-266 (1996).